



## Article

# Grinding Test on Tremolite with Fibrous and Prismatic Habit

Oliviero Baietto , Mariangela Diano, Giovanna Zanetti  and Paola Marini

Department of Environment, Land and Infrastructure Engineering (DIATI), Politecnico di Torino, 10129 Turin, Italy; mariangela.diano92@gmail.com (M.D.); giovanna.zanetti@polito.it (G.Z.); paola.marini@polito.it (P.M.)

\* Correspondence: oliviero.baietto@polito.it

Received: 16 April 2019; Accepted: 20 May 2019; Published: 1 June 2019



**Abstract:** The main objective of this work is the evaluation of the morphology change in tremolite particles before and after a grinding process. The crushing action simulates anthropic alteration of the rock, such as excavation in rocks containing tremolite during a tunneling operation. The crystallization habit of these amphibolic minerals can exert hazardous effects on humans. The investigated amphibolic minerals are four tremolite samples, from the Piedmont and Aosta Valley regions, with different crystallization habits. The habits can be described as asbestiform (fibrous) for longer and thinner fibers and non-asbestiform (prismatic) for prismatic fragments, also known as “cleavage” fragments. In order to identify the morphological variation before and after the grinding, both a phase contrast optical microscope (PCOM) and a scanning electron microscope (SEM) were used. The identification procedure for fibrous and prismatic elements is related to a dimensional parameter (length–diameter ratio) defined by the Health and Safety Executive. The results highlight how mineral comminution leads to a rise of prismatic fragments and, therefore, to a potentially safer situation for worker and inhabitants.

**Keywords:** tremolite; Naturally Occurring Asbestos (NOA); asbestos; grinding test; PCOM; image analysis

## 1. Introduction

The object of this study is tremolite, a hydrated calcium magnesium silicate ( $\text{Ca}_2\text{Mg}_5\text{Si}_8\text{O}_{22}(\text{OH})_2$ ), belonging to the tremolite-ferro-actinolite series [1,2], with an amphibolic structure characterized by long and parallel double chains of silica tetrahedral ( $\text{SiO}_4$ ) with a strip of cations located between the double chains [2–6].

Tremolite and actinolite can crystallize with two different crystalline habits and it is common to find them in fibrous habit, known as asbestiform, or in prismatic habit, non-asbestiform. This distinction can be described as [7]:

- “Asbestiform habit” is associated with a crystalline structure characterized by thin crystals similar to the morphology of organic fibers (hair; the resemblance is not in the width,  $10^{-6}$  m for asbestos fibers vs  $10^{-5}$  m for hair) or as a crystalline aggregation consisting of parallel fibers (bundles with indented extremities). The fibers are thin, long, and similar to needle-shaped elements with a unidirectional growth [8].
- “Non-asbestiform” refers to a structure characterized by tiny or “elongated prisms with a lozenge-shaped cross section” [4]. The crystalline growth is not unidirectional.

A crushing event acting on tremolite crystals could have different effects on crystalline habits, as illustrated by Illgren et al. [5]. In fact, amphiboles with asbestiform habits have a significant propensity to be longitudinally split. The longitudinal separation produces “fibrils” that are thinner and thinner without any perpendicular breakup to the elongation; therefore, fibers maintain their flexibility and tensile strength [4,5,9]. Non-asbestiform habits, however, consist of amphibolic minerals with internal cleavage. This term relates to the fact that breakage occurs along preferential planes, especially planes of relative weakness, and mainly perpendicular to the length [5,7]. The prismatic elements have, therefore, a tendency to fracture along these preferential planes, producing stocky prisms or acicular fragments with a reduction in their flexibility.

The particle morphology, size, physical–chemical properties and biopersistence correlated to the crystalline habits can involve relevant consequences to the human respiratory system. The Italian Minister of Health [10] highlighted the difficult removal process for asbestiform amphiboles, caused by the length and persistence of the fiber. These fibers are stronger and more flexible than cleavage fragments, so they tend to bend without breaking and also have negative repercussions on the defense mechanism operated by macrophages. Otherwise, Illgren et al. [5] specified that non-asbestiform (or prismatic) amphiboles have weaknesses and fragile behavior. Therefore, the prismatic component can be reduced into fragments that can progressively be cleared from the body by the macrophage phagocytosis.

Asbestos is included in Group 1, referring to “substances carcinogenic to humans”, by the International Agency for Research on Cancer (IARC). It is important that the concept of regulated asbestos fibers, which correspond to fibers defined as “respirable” by the World Health Organization (WHO) (fibers having length  $> 5 \mu\text{m}$ , diameter  $\leq 3 \mu\text{m}$ , and length/diameter (aspect) ratio  $\geq 3:1$ ) [11–13]. For this reason, many trials were focused on the evaluation of the carcinogenic effect, such as the potential for mesothelioma induction, for a non-asbestiform tremolite by means of in vivo (animals or human) and in vitro tests. These studies, seen in Table 1, demonstrate a negative or lower rate of carcinogenicity for non-asbestiform tremolite compared to asbestiform tremolite.

**Table 1.** Carcinogenic experiment on asbestiform and non-asbestiform tremolite.

Test Subjects		Procedure	Authors
Workers		Exposure to non-asbestiform tremolite	Gamble et al. [2]
In vitro		Test by a variety of cellular endpoints	Timbrell et al. [14]
			Wylie & Mossman [15] Wagner et al. [16]
In vivo (such as rat)	Experiment:	Inhalation	Davis et al. [17]
		Intraperitoneal or intrapleural injection	Wagner et al. [18]
			Smith et al. [19]
			Davis et al. [20]
		Intrapleural implant	Stanton et al. [21]

This introduction about tremolite habits and their behavior is directly connected with the purpose of this research: the evaluation of the grinding effect on the morphology of four tremolite samples. This study aims to analyze the morphological changes of both the fibrous and the prismatic states in order to simulate the external process of rock deterioration. The grinding effect strictly depends on both the characteristics of asbestos mineral (rocks cohesion and friability) and interaction of the rock with external “phenomena”. In the last year the effect of grinding on tremolite asbestos has been well investigated by Bloise et al. [22] (2018). In this work, the study focuses not only on asbestiform samples but on prismatic tremolite too. This decision arises from the need to verify if the tremolite with prismatic habit, if subjected to a grinding process, can produce potentially harmful fibers. These events can happen during natural degradation processes of rocks (weathering of outcrops) or during anthropic intervention, such as the mechanized excavation or earthmoving process (transport). These processes, which employ a series of crushing and abrasive actions on the rock, are the cause of dimensional

reduction of asbestos fibers, where present, and therefore can provoke serious human health problems linked to the release of fibers in air or in groundwater, so entering in the hydrological system [23].

The results showed increases in prismatic elements for all tremolite samples after grinding. Regarding the carcinogenetic studies previously proposed, the increase of prismatic particles could lead to a safer situation in term of reducing impact on both the health of exposed humans (workers, inhabitants, and health professionals) and on the economy and organization for mining companies operating in deposits where a non-asbestos tremolite is present [2].

## 2. Materials and Methods

Four samples of tremolite were collected in four sites from the north of Italy—three in the Piedmont region (Bracchiello, Monastero di Lanzo, and Caprie) and the last in Aosta Valley (Verrayes). These tremolites showed different initial habits: prismatic for Bracchiello, Caprie, and Verrayes; fibrous for Monastero. For each sample, the particle morphology was investigated before and after grinding, with both a phase contrast optical microscope (PCOM) and a scanning electron microscope (SEM). A counting strategy to differentiate the asbestiform fibers from the non-asbestiform particles was chosen. This approach was focused on a dimensionless parameter, mainly the ratio between length and diameter ( $L/D$ ), acquired during the PCOM observation, according to the asbestiform definition of the Health and Safety Executive in which an  $L/D > 20$  identifies a particle as fibrous [24].

### 2.1. Material


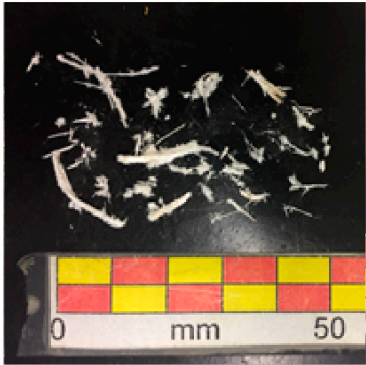

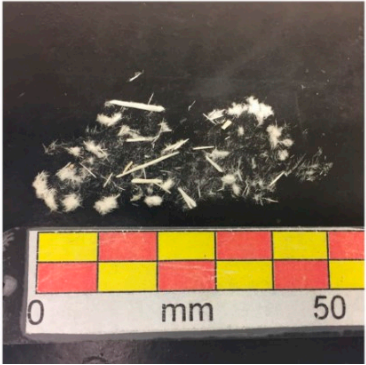
The four samples of tremolite analyzed were from Piedmont and Aosta Valley. More precisely, three of four came from Piedmont: Bracchiello (TO), Monastero di Lanzo (TO), and Caprie (TO). The other one, from Aosta Valley, was Verrayes (AO). The samples were collected by Prof. C. Clerici and are part of the mineralogic museum of DIATI.

The sample characteristics are shown in Figure 1.

### 2.2. Phase Contrast Optical Microscope (PCOM)

The PCOM (Leica Microsystem, Wetzlar, Germany) used was a LEICA Phase Contrast DLMP equipped with 10×, 20× and 40× lenses and a Leica DFC290 digital camera [25]. In order to analyze the material, a small amount of sample was prepared on a microscopic slide and immersed in a high-dispersion liquid with a known refraction index. This refractive index oil affects three parameters: (1) luminosity, (2) color, and (3) birefringence [25–27].

Luminosity is closely connected to the luminance contrast. This means that the brightness ratio between an object and its immediate background depends on an oil with a known refractive index. The color, both of the particle and the surrounding halo, is obtained when the difference between the refractive index of liquids and particles ( $\Delta n = n_l - n_p \approx 0$ ) is within the range  $-0.020$ – $0.020$ . The chromatic effect that arises for different  $\Delta n$  and different  $K$  (ratio between the slope of the chromatic curves of liquids and solids) is shown in Figure 2, where the color reported above refers to the color of the particle, while the one below refers to the color of the surrounding halo [28].

Sample nomenclature	Aspect	Characteristic
Bracchiello - Bracchiello (TO)		Particles have variable length in the 1–10 mm range and present a rectilinear and rigid aspect (not flexible). They also appear translucent and not aggregate.
Monastero - Monastero di Lanzo (TO)		Particles appear aggregated in bundles. This is the only sample that presents a fibrous aspect. Thus, particles have an apparent flexibility and the bundles have frayed extremities.
Caprie - Caprie (TO)		Particles have variable length in the 1–10 mm range. These are prismatic with a rigid and scattered aspect. There is a clear, high quantity of fine components.
Verrayes - Verrayes (AO)		Particles have extreme variability in length and thickness. Prismatic fragments and fine components are noticeable; only the latter are scattered or aggregated in a small mass. There is a clear, high quantity of fine components.

**Figure 1.** Aspect and characteristics of the samples.

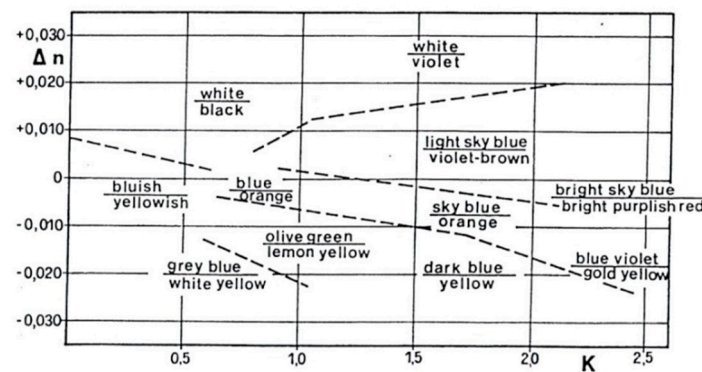


Figure 2. Table of color effects [28] published by Staub, 1955.

### 2.3. Scanning Electron Microscope (SEM)

The SEM used was a FEI (FEI Company, Hillsboro, OR, USA) operating at 5 and 20 kV. This technology has a resolution of 0.01  $\mu\text{m}$ , for conductive samples, in contrast to the 0.25  $\mu\text{m}$  resolution of the PCOM [25,29]. In this case the resolution of the SEM depends on the grain size of the sputtered coating material (gold) because asbestos is a non-conductive material. It has been used to acquire qualitative images that are subsequently compared with those obtained from the PCOM.

### 2.4. Methodology

A schematic description of the analysis methodology is reported in Figure 3. For each original sample, two microscopic analyses were carried out: the first on the original samples and the second on the ground samples. The main action of this analysis is to submit both original and ground samples to counting and measuring using the PCOM. SEM was used for a visual comparison to PCOM images.

All the steps will be illustrated in the following subsection.

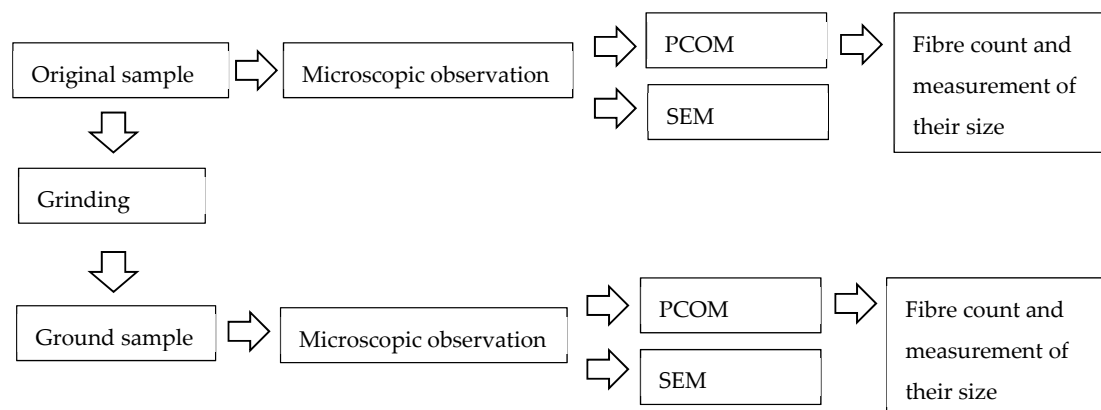


Figure 3. Analysis procedure flowsheet.

#### 2.4.1. Sample Preparations for Microscopic Observation

The first analysis step consisted of the preparation of samples for observation with PCOM and SEM. This action was carried out both for the natural samples and the ground samples.

For the PCOM observation, a portion of the sample was placed on a microscopic slide and immersed in a refractive index oil. To recognize a tremolite asbestos, a liquid with a refraction index equal to 1.615 is suggested [30]. In this study, a liquid with a refraction index of 1.600 was used. This value, slightly lower than the refraction index of the investigated material, allows a maximum contrast between tremolite crystals and the background, reducing the chromatic effect and the halo surrounding the particles. This optical condition is useful for observing the particles with image software programs.



The sample weight must only be considered indicative of a good PCOM observation and particle measurement. In Table 2, the quantity, in milligrams, of material located on the slide is shown.

**Table 2.** Amount of material on the microscopic slide for each sample.

Sample Nomenclature	Natural Sample (mg)	Ground Sample (mg)
Bracchiello	0.6	0.3
Monastero	0.2	0.3
Caprie	0.3	0.3
Verrayes	0.3	0.3

For SEM observation, the sample must be attached to a stub; each sample was prepared by mixing 10 mg of material in 200 mL of deionized water. Subsequently, 7.5 mL of this mixture was filtered on a polycarbonate membrane (0.4  $\mu$ m porosity) and fixed on a metallic stub. After that, the specimen must be coated with a thin layer of gold, essentially to abate the increase of high-voltage charges on the specimen and dangerous heat [31].

#### 2.4.2. Grinding

The tremolite behavior after a grinding process was studied by subjecting an amount of original sample, approximately 700 mg, to grinding for 1 minute in an agate jar closed with a sealing gasket lid (model number 952/2 from Humboldt-Wedag). The jar had a hardness of 7.0 Mohs and its dimensions were: diameter of 109 mm, height of 55 mm, and maximum volume of filling of 30 mL.

The fundamental characteristics of the engine's mill were a power of 200 W and a voltage of 230 V/50 Hz. The jar was perfectly fixed and the movement of the crusher was oscillating with eccentric mass.

All the steps of the analysis procedure, such as the selection of the sample, the extraction of the grinding material from the jar, and the preparation of the sample for observation, may lead to a potential exposure to tremolite fibers. Therefore, all steps were carried out using adequate protection devices and under a fume hood (Black Activa Plus from Aquaria).

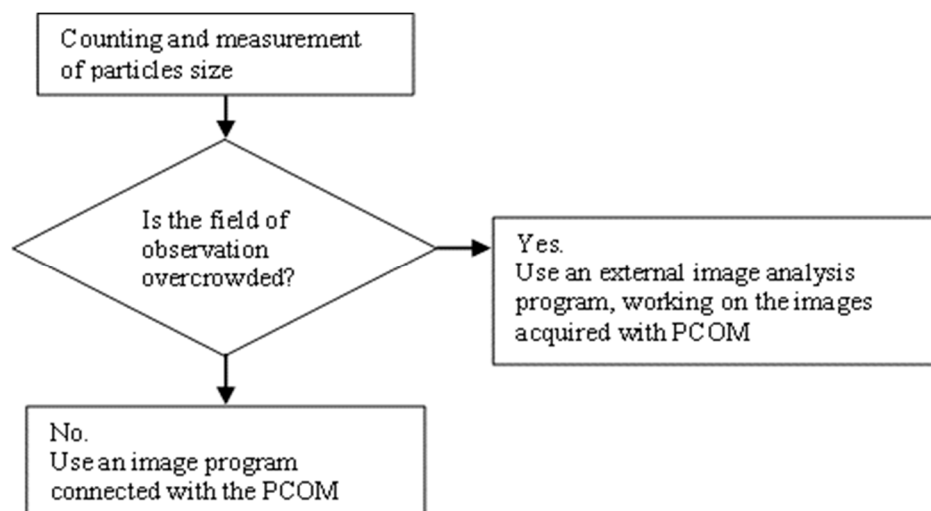
#### 2.4.3. Decision-Making Processes for Counting and Measurement of Particles

The counting and measurement of each particle were carried out on PCOM images. Eight sample slides were analyzed, four belonging to the original samples and the other four to the grinding samples. For each slide, the number of observation fields had to be selected, as shown in Table 3, and this depended on the object dimensions.

**Table 3.** Number of fields examined and particles counted for each sample.

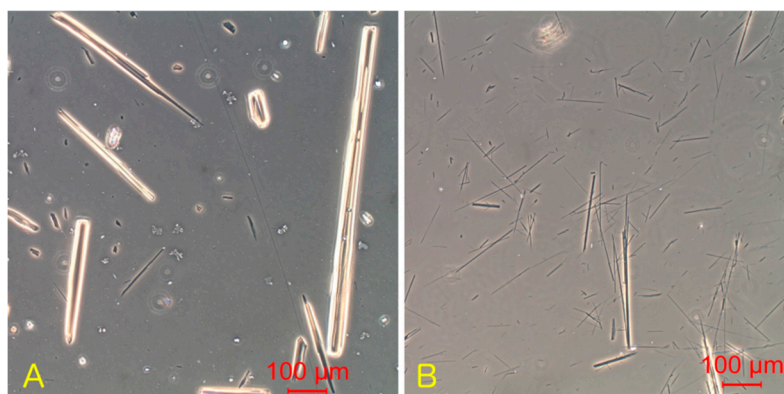
Sample Nomenclature	Original Sample		Ground Sample	
	Number of Fields Examined	Number of Particles Counted	Number of Fields Examined	Number of Particles Counted
Bracchiello	100	240	36	331
Monastero	10	2929	25	358
Caprie	100	669	25	288
Verrayes	25	562	25	458

The number of fields investigated differed considerably among the original samples, mainly due to the different dimensions of the particles. A 10 $\times$  objective has been used for original samples, while a 40 $\times$  objective for the ground samples. Length and width of particles were measured for each field. The decision-making process is illustrated in Figure 4.



**Figure 4.** Decision-making process for particle counting and measurement on phase contrast optical microscope (PCOM). Relationship with the field of observation overcrowding.

More precisely, in the case of readable fields of observation (not crowded), real-time measurements were made directly on the image coming from the microscope camera to a monitor. In crowded fields, all the acquired images were instead studied offline with a free image processing software, ImageJ, and both length and thickness were measured. In Figure 5, two images are shown to illustrate field overcrowding, which affected the decision-making process.



**Figure 5.** Examples of field crowding for counting and measuring elements: (A) Readable field, (B) crowded field.

Crystalline particles can be categorized as:

- Fibrous: long and thin fibers;
- Prismatic: elements with a significant thickness and flatness (resulting from planar rupture) or acicular extremities;
- Acicular: long and thin fibers with at least one needle-shaped end;
- Bundle of fibers: indistinguishable elements inside a bundle, where one exists.

The dimensional distinction between fibrous (asbestiform) and prismatic (non-asbestiform) components was made according to the Health and Safety Executive [24]. For HSE “the asbestiform habit is recognized by the following characteristics:

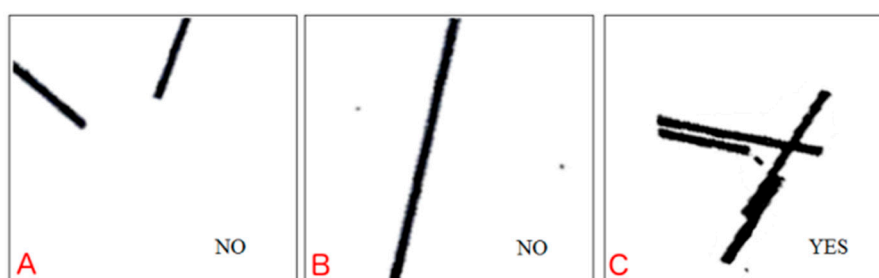
- A range of aspect ratios ranging from 20:1 to 100:1 or higher for fibers longer than 5  $\mu\text{m}$ ;
- The capability of splitting into very thin fibrils;

- Two or more of the following:
  - Parallel fibers occurring in bundles;
  - Fiber bundles displaying frayed ends;
  - Fibers in the form of thin needles;
  - Matted masses of individual fibers; and/or
  - Fibers showing curvature.”

#### 2.4.4. Closing Remarks on the Counting and Measurement of Particles

The counting and measurement of particles in each field were realized based on the following considerations:

- Only crystalline elements falling within the outline of the microscopic reticle, and not the particles exceeding this area, have been considered, as shown in Figure 6;
- The fields of observation are casually selected inside the coverslip, more precisely following a grid and each field is not repeatable;
- During the measurement, fiber and/or fragment elements having length  $> 5 \mu\text{m}$ , without any restriction in the diameter, have been included;  $5 \mu\text{m}$  is a threshold coming from the regulated fibers definition ( $>5 \mu\text{m}$  in length,  $\leq 3 \mu\text{m}$  in diameter width, length/diameter (aspect) ratio  $\geq 3:1$ ) according to the World Health Organization and adopted in the Italian Minister Decree 06.09.94 [13,29]. It was chosen to not use the diameter threshold because we needed to measure the width of prismatic components, which are much greater than  $3 \mu\text{m}$ ;
- Particles are individually counted but, in the case of a bundle of crystalline elements, where these touch or cross each other it was counted as one fiber;
- In a prismatic fragment, which appears acicular or irregular at one or more point of its length, the diameter is measured along the section. This chosen section must not be influenced by breakage;
- A sufficient number of fields to reach the hundreds of elements were observed.



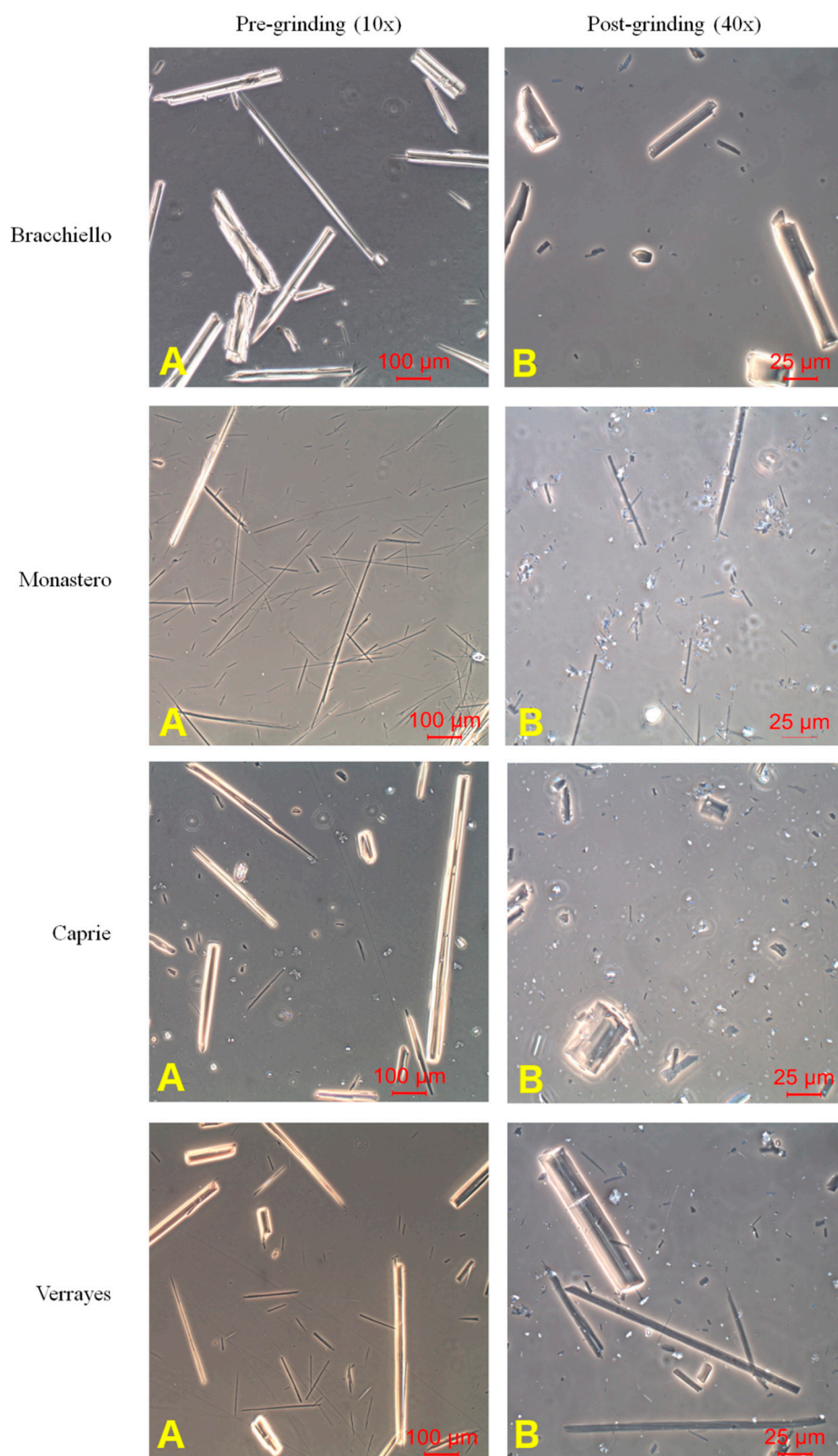
**Figure 6.** Particle counting: (A,B) If the elements are cut by the outline of the microscopic reticle, these will be discarded, and (C) if the elements fall within the outline of the microscopic reticle, these will be considered [24].

### 3. Results

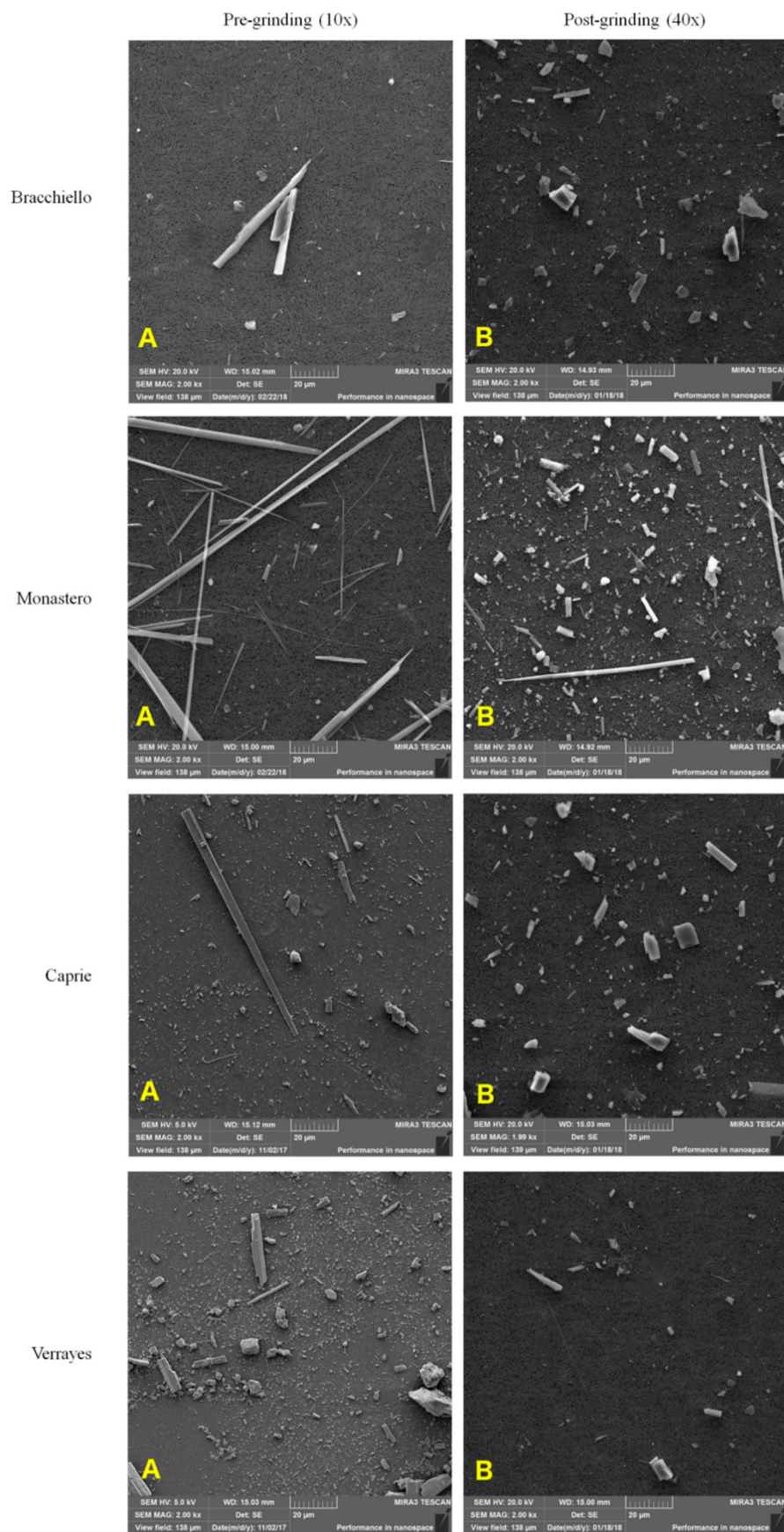
Table 4 summarizes all the information about the preparation and observation of samples, ground or not, using PCOM.

Figure 7, PCOM, and Figure 8, SEM, contain the most significant images for both the original and ground samples to give a visual comparison.





**Figure 7.** PCOM images (A) before and (B) after grinding.



**Figure 8.** Scanning electron microscope (SEM) images, before (A) and after grinding (B).

**Table 4.** Summarized information about original and ground samples.

Original samples	Sample nomenclature	Bracchiello	Monastero	Caprie	Verrayes
	Weight on slide (mg)	0.6	0.2	0.3	0.3
	PCOM objective	10×	10×	10×	10×
	Refractive index of oil	1550	1600	1600	1600
	Fields of observation	100 fields (20 × 5 strips)	20	100 fields (20 × 5 strips)	25
	Coverslip area (mm <sup>2</sup> )	25 × 25	34 × 40	25 × 25	25 × 25
	Number of particles analyzed	240	2929	669	526
Ground samples	Sample nomenclature	Bracchiello	Monastero	Caprie	Verrayes
	Weight on slide (mg)	0.3	0.3	0.3	0.3
	PCOM objective	40×	40×	40×	40×
	Refractive index of oil	1600	1600	1600	1600
	Fields of observation	25	25	25	25
	Coverslip area (mm <sup>2</sup> )	25 × 25	25 × 25	25 × 25	25 × 25
	Number of particles analyzed	331	358	288	458

The charts in Figure 9 show the results of the granulometric analysis, more precisely the trend in particle length before and after the grinding process. These graphs are frequency histograms, where each class of length is related to its frequency (%). A 5 µm minimum value for length has been chosen according to the minimum value in the respirable fiber definition from WHO [18]. For each class of length, the peak height is defined by the percentage frequency (%) as:

$$\%_i = \frac{(n.of\ fibers)_i}{total\ number\ of\ fibres\ observed} \cdot 100, \quad (1)$$

where  $i$  is the  $i$ th class of length.

The difference in colors adopted in the graphs shown in Figure 9 helps to recognize the two steps of analysis: yellow for the original samples and green for the ground samples.

The bar charts in Figure 10 illustrate the difference between fibrous and prismatic components before and after grinding based on the Health and Safety Executive definition [29]. A fiber is a component with a length–diameter ratio higher than 20, otherwise, it can be considered a prism.

Therefore, the number of fibrous ( $L/D > 20$ ) and prismatic ( $L/D < 20$ ) components were determined for the two-step analysis and their percentage frequency was defined as follows:

$$\%_i fibrous = \frac{(n.\ of\ fibers\ with\ \frac{L}{D} > 20)_i}{(total\ number\ of\ fibres\ observed)_i} \cdot 100, \quad (2)$$

$$\%_i prismatic = \frac{(n.\ of\ fibers\ with\ \frac{L}{D} < 20)_i}{(total\ number\ of\ fibres\ observed)_i} \cdot 100, \quad (3)$$

where  $i$  is the  $i$ th status of the sample (original or ground).



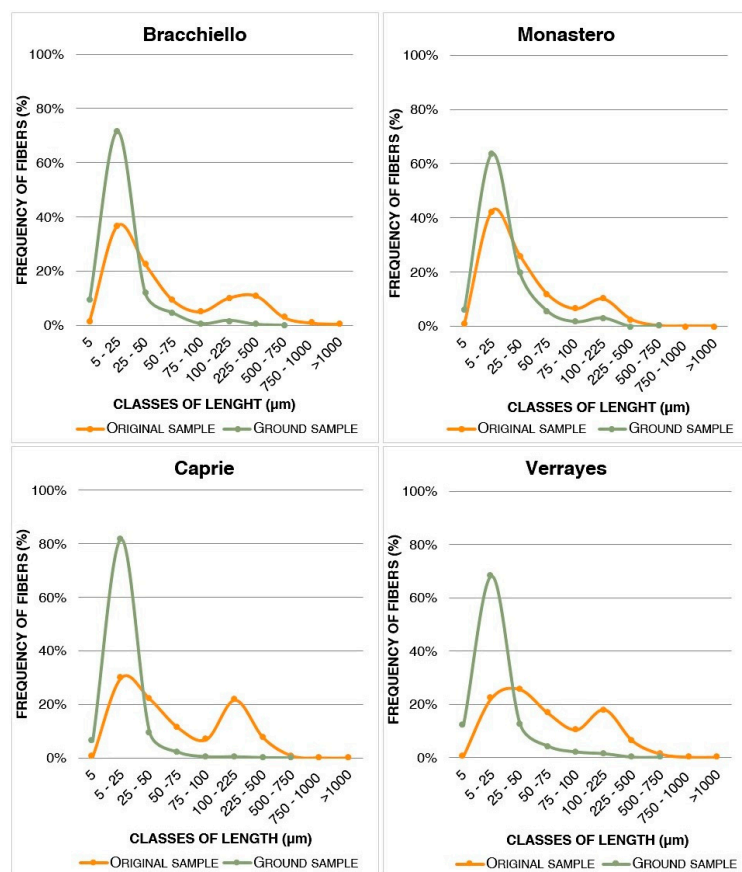


Figure 9. Percentage frequency of particles in each sample, before and after grinding.

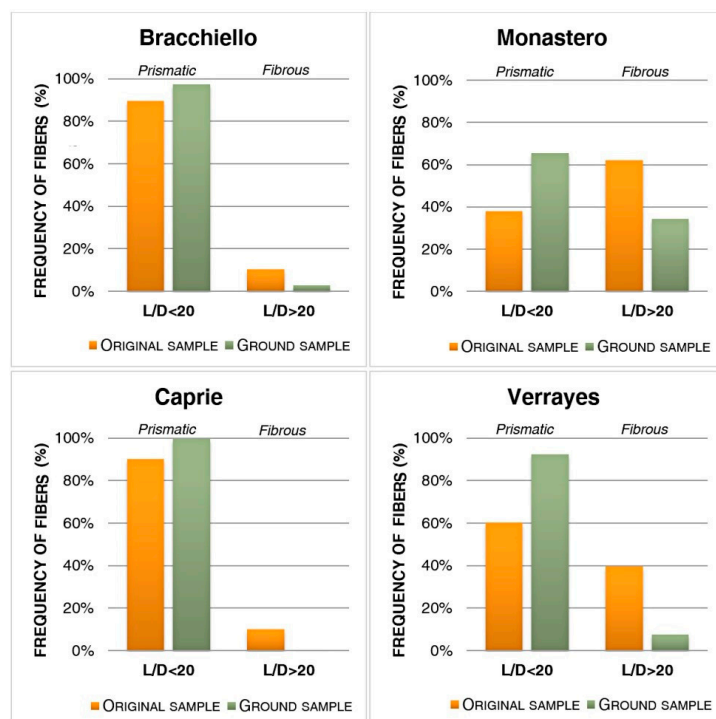


Figure 10. Amounts of fibrous and prismatic component according to the Health and Safety Executive (HSE) [23] before and after grinding.

## 4. Discussion

### 4.1. Granulometric Analysis

The results from the granulometric analysis, shown in Figure 9, demonstrate a similarity in the reduction of component length. The original samples are characterized by a great frequency of particles located in the 5–25  $\mu\text{m}$  and 100–225  $\mu\text{m}$  classes. These two classes delineate two obvious peaks and there is one in the 75–100  $\mu\text{m}$  class with a lower frequency. The grinding action is shown by the green curve. This process highlights an attenuation of the second peak (100–225  $\mu\text{m}$ ) and a growth in the first (5–25  $\mu\text{m}$ ). The long components have a reduction of their length and there is an increase of short elements inside the 5–25  $\mu\text{m}$  class. In short, particles undergo a break perpendicular to the length during grinding and this action causes a reduction of their length. This case is different from the classic asbestos breaking method, which is defined as a longitudinal split of the fibers.

The elements with lengths lower than 5  $\mu\text{m}$  were not considered, because they are not covered in the definition of a respirable fiber by the World Health Organization [13]. The graphs in Figure 6 show a high concentration of ground particles around 25  $\mu\text{m}$ . The maximum diameter is 2.5  $\mu\text{m}$ , ten times higher than the limits of PCOM. Therefore, PCOM is a reliable instrument for this kind of analysis. Moreover, the SEM analysis on the ground samples has permitted checking of the accuracy of the previous analysis. This is especially valuable to avoid errors related to the particle dimensions.

### 4.2. Dimensional Analysis Based on the Health and Safety Executive Definition

The results of the dimensional analysis, shown in Figure 10, illustrate the variation in the fibrous and prismatic components before and after the grinding process. Looking at the original sample, the yellow bars, Bracchiello and Caprie present more accentuated prismatic components in comparison to the Verrayes sample. The Monastero sample is characterized by the presence of a fibrous component. After the grinding process (the green bars) there is a % decrease of the fibrous elements, with a consequent increase of the prismatic component, which is especially marked for Verrayes and Monastero (decreases of 32% and 27%) and slight for Caprie and Bracchiello (decreases of 9% and 6%).

## 5. Conclusions

The aim of this study was the evaluation and analysis of tremolite behavior submitted to anthropic (or natural) mechanical actions, which subsequently contribute to the release of fibers into the environment. It is important to underline that tremolite in nature can be present in two crystalline habits: asbestiform (fibrous) or non-asbestiform (prismatic). Therefore, the objective is pointed towards the evaluation of morphology changes in fibers or prism particles after a grinding process. The dimensional analysis, which is based on a direct measurement of the particle size (length and diameter), has allowed the study of these changes by means of the definition from the Health and Safety Executive. HSE distinguishes the fibrous component from the prismatic using the ratio between length and diameter ( $L/D$  higher than 20 defines a particle as fibrous).

The results of this research indicate that the prevalent morphology of an amphibolic mineral (in this case, a tremolite asbestos) can change habit. This is the case for the Monastero sample, which initially appeared fibrous but after the grinding process its fibrousness was reduced because the production of prismatic elements took over. The other samples, which initially contained a high content of prismatic particles, were subject to further increases in their prismaticity. The dimensional analysis allowed realistic and reliable results to be obtained for both the samples' composition and for the effects of grinding.

Regarding the carcinogenicity aspects of asbestos, the production of prismatic components in an amphibolic mineral by means of grinding action (digging or earthmoving), can generally be a safer situation for the exposed subjects, such as workers and inhabitants. This is an interesting theme focused on the relationship between the crystalline particle breaking methods and their impact on the respiratory system. In fact, as previously exposed, many experimental studies carried out by



different authors proved a lower rate of carcinogenicity for a non-asbestiform amphibole than an asbestiform amphibole.

This study can be used for future surveys, in application to another typology of amphibolic minerals, such as actinolite, and comparing an asbestiform mineral with a non-asbestiform one. Furthermore, it would be also interesting and useful to provide an evaluation about the potential effects on human health and, therefore, obtain a correspondence with the other authors in term of carcinogenicity of these non-asbestiform tremolites.

**Author Contributions:** Conceptualization: O.B., M.D., P.M. and G.Z.; Data curation: M.D.; Methodology: O.B. and Giovanna Zanetti; Supervision: P.M.; Writing—original draft: M.D.; Writing—review & editing: O.B. and P.M.

**Funding:** This research received no external funding.

**Conflicts of Interest:** The authors declare no conflict of interest.

## References

- Deer, W.A.; Howie, R.A.; Zussman, J. *An Introduction to the Rock Forming Minerals*, 1st ed.; Longman Group Limited: London, UK, 1966.
- Gamble, J.F.; Gibbs, G.W. An evaluation of the risks of lung cancer and mesothelioma from exposure to amphibole cleavage fragments. *Regul. Toxicol. Pharmacol.* **2008**, *52*, S154–S186. [[CrossRef](#)] [[PubMed](#)]
- Roggli, V.L.; Vollmer, R.T.; Butnor, K.J.; Sporn, T.A. Tremolite and mesothelioma. *Ann. Occup. Hyg.* **2002**, *45*, 447–453.
- Addison, J.; McConnell, E.E. A review of carcinogenicity studies of asbestos and non-asbestos tremolite and other amphiboles. *Regul. Toxicol. Pharmacol.* **2008**, *52*, S187–S199. [[CrossRef](#)] [[PubMed](#)]
- Ilgren, E.B.; Penna, B.M. The biology of cleavage fragments: A brief synthesis and analysis of current knowledge. *Indoor Built Environ.* **2014**, *13*, 343–356. [[CrossRef](#)]
- Ross, M.; Langer, A.M.; Nord, G.L.; Nolan, R.P.; Lee, R.J.; Orden, D.V.; Addison, J. The mineral nature of asbestos. *Regul. Toxicol. Pharmacol.* **2008**, *52*, S26–S30. [[CrossRef](#)] [[PubMed](#)]
- National Research Council. *Asbestiform Fibers: Nonoccupational Health Risks*; National Academies Press: Washington, DC, USA, 1984.
- Dana, S.D.; Ford, W.E. *A Textbook of Mineralogy*; Wiley and Sons: New York, NY, USA, 1932.
- Dorling, M.; Zussman, J. Characteristics of asbestiform and non-asbestiform calcic amphiboles. *Lithos* **1987**, *20*, 469–489. [[CrossRef](#)]
- Ministero della Salute Italiana. Sintesi delle conoscenze relative all'esposizione e al profilo tossicologico-Amianto. Available online: [http://www.salute.gov.it/imgs/C\\_17\\_pubblicazioni\\_2570\\_allegato.pdf](http://www.salute.gov.it/imgs/C_17_pubblicazioni_2570_allegato.pdf) (accessed on 27 May 2019).
- IARC. Some inorganic and organometallic compounds. *IARC Monogr. Eval. Carcinog. Risk Chem. Man.* **1973**, *2*, 1–181.
- Gualtieri, A.F.; Gandolfi, N.B.; Pollastri, S.; Rinaldi, R.; Sala, O.; Martelli, G.; Bacci, T.; Paoli, F.; Viani, A.; Viglitturo, R. Assessment of the potential hazard represented by natural raw materials containing minerals fibers—The case of the feldspar from Orani, Sardinia (Italy). *J. Hazard. Mater.* **2018**, *350*, 76–87. [[CrossRef](#)]
- International Programme on Chemical Safety & WHO Task Group on Asbestos and other Natural Mineral Fibers. *Asbestos and Other Natural Mineral Fibers/Published under the Joint Sponsorship of the United Nations Environment Programme*; World Health Organization: Geneva, Switzerland, 1986; Available online: <http://www.who.int/iris/handle/10665/37190> (accessed on 27 May 2019).
- Timbrell, V.; Griffiths, D. Pooley, Possible importance of fiber diameters of South African Amphiboles. *Nature* **1971**, *232*, 55–56. [[CrossRef](#)]
- Wylie, A.; Mossman, B. Mineralogical features associated with cytotoxic and proliferative effects of fibrous talc and asbestos on tracheal epithelial and pleural mesothelial cells. *J. Toxicol. Appl. Pharmacol.* **1997**, *147*, 143–150. [[CrossRef](#)]
- Wagner, J.C.; Chamberlain, M.; Brown, R.; Berry, G.; Pooley, F.; Davies, R.; Griffiths, D. Biological effect of tremolite. *Br. J. Cancer* **1982**, *45*, 352–371. [[CrossRef](#)]
- Davis, J.M.G.; Addison, J.; Bolton, R.E.; Donaldson, K.; Jones, A.D.; Miller, B.G. Inhalation studies on the effects of tremolite and brucite dust in rats. *Carcinogenesis* **1985**, *6*, 667–674. [[CrossRef](#)] [[PubMed](#)]

18. Wagner, J.C.; Slegs, C.; Marchands, P. Diffuse pleural mesothelioma and asbestos exposure in the North Western Cape Province. *Br. J. Ind. Med.* **1960**, *17*, 260–271. [[CrossRef](#)] [[PubMed](#)]
19. Smith, W.; Hubert, D.; Sobel, H.; Marquet, E. Biologic tests of tremolite in hamsters. In *Dust and Disease, proceedings of the Conference on Occupational Exposures to Fibrous and Particulate Dust and Their Extension into the Environment, Washington, DC, USA, 1977*; Pathotox Publishers: Park Forest South, IL, USA, 1979; pp. 335–339.
20. Davis, J.M.G.; Addison, J.; McIntosh, C.; Miller, B.; Niven, K. Variations in the carcinogenicity of tremolite dust samples of differing morphology. *Ann. N. Y. Acad. Sci.* **1991**, *643*, 473–483. [[CrossRef](#)]
21. Stanton, M.; Layard, M.; Tegeris, A.; Miller, E.; May, M.; Morgan, E.; Smith, A. Relation of particle dimension to carcinogenicity in amphibole asbestos and other fibrous minerals. *J. Natl. Cancer Inst.* **1981**, *67*, 965–975.
22. Bloise, A.; Kusiorowski, R.; Gualtieri, A. The effect of grinding on tremolite asbestos and anthophyllite asbestos. *Minerals* **2018**, *8*, 274. [[CrossRef](#)]
23. Gualtieri, A.F.; Pollastri, S.; Gandolfi, N.B.; Ronchetti, F.; Albonico, C.; Cavallo, A.; Zanetti, G.; Marini, P.; Sala, O. Minerals in the human body—Determination of the concentration of asbestos minerals in highly contaminated mine tailings: An example from abandoned mine waste of Crètaz and Èmarese (Valle d’Aosta, Italy). *Am. Mineral.* **2014**, *99*, 1233–1247. [[CrossRef](#)]
24. Health and Safety Executive. *Asbestos: The Analysts’ Guide for Sampling, Analysis and Clearance Procedures*; HSE Books: Norwich, UK, 2005.
25. Baietto, O.; Marini, P. Naturally occurring asbestos: Validation of PCOM quantitative determination. *Resour. Policy* **2018**, *59*, 44–49. [[CrossRef](#)]
26. Clerici, C.; Morandini, A.; Occella, E.; Visetti, A. L’impiego del contrasto di fase in microscopia. *Boll. dell’associ. Miner. Subalp.* **1975**, *12*, 268–298.
27. Niskanen, L.; Rätty, J.; Peiponen, K.E. Determination of the refractive index of microparticles by utilizing light dispersion properties of the particle and an immersion liquid. *Talanta* **2013**, *115*, 68–73. [[CrossRef](#)] [[PubMed](#)]
28. Schmidt, K.G. Die phasenkontrastmikroskopie in der staubtechnik. *Staub* **1955**, *41*, 436.
29. Marconi, A. L’identificazione delle fibre di asbesto per mezzo della tecnica microscopica della dispersione cromatica. *Ann. dell’Ist. Super. Della Sanità* **1982**, *18*, 911–914.
30. Decreto del Ministero della Sanità 6 settembre 1994: Normative e metodologie tecniche di applicazione dell’art. 6, comma 3, e dell’art. 12, comma 2, della legge 27 marzo 1992, n. 257, relativa alla cessazione dell’impiego dell’amianto. (GU Serie Generale n.220 del 20-09-1994 - Suppl. Ordinario n. 129. Available online: [https://www.unipd-org.it/rls/pericolirischi/Pericoli/.../d.m.\\_06.09.94.pdf](https://www.unipd-org.it/rls/pericolirischi/Pericoli/.../d.m._06.09.94.pdf) (accessed on 28 May 2019).
31. Bozzola, J.J.; Russell, L.D. *Electron. Microscopy: Principles and Techniques for Biologists*, 2nd ed.; Jones & Bartlett Learning: Burlington, MA, USA, 1992.



© 2019 by the authors. Licensee MDPI, Basel, Switzerland. This article is an open access article distributed under the terms and conditions of the Creative Commons Attribution (CC BY) license (<http://creativecommons.org/licenses/by/4.0/>).